JOURNAL OF PROPULSION AND POWER
Vol. 12, No. 2, March–April 1996

Transcritical Liquid Oxygen Droplet Vaporization: Effect on Rocket Combustion Instability

J.-P. Delplanque* and W. A. Sirignano†
University of California, Irvine, Irvine, California 92717

The response of a liquid oxygen droplet to oscillatory ambient conditions consistent with liquid-rocket engines over a wide range of frequencies is computed. Two configurations are considered: 1) isolated droplets and 2) droplets in an array. The consequences of nonuniformities introduced in the gas phase by neighboring droplets on the droplet response are evaluated. The potential of gasification as the rate-controlling mechanism was evaluated through the computation of a response factor derived from the Rayleigh criterion. Computations show that the peak frequency for the computed response factor is mainly correlated to the droplet lifetime and also depends on the type of flow that the droplet is experiencing (with or without reversal). Consequently, droplet secondary atomization, which causes a substantial droplet lifetime reduction, induces a significant (one order of magnitude) shift in the peak frequency. As a result, the frequency of the maximum response factor is too high to correspond to the acoustic frequencies of the typical modes for standard cryogenic rocket engine chambers. Since droplets are likely to undergo secondary atomization in the stripping regime for most of their lifetime in these engines, this phenomenon explains the observed better stability of such engines compared to storable propellant engines. It was also shown that the droplet gasification process, whether undergoing stripping or not, can drive combustion instabilities for the longitudinal mode, under certain simplifying assumptions. The effects of mean pressure and pressure fluctuations on the droplet response were also evaluated.

Nomenclature

a = speed of sound
C_p, C_v = specific heats
f = frequency
G = gasification response factor
G_e = elementary response factor
n = interaction index
P = pressure
T = temperature
t = time
t_{life} = droplet lifetime
U = velocity
$\dot{W}$ = gasification rate
x = spatial coordinate
ε_ψ = relative amplitude fluctuation of ψ
λ = wavelength
τ = sensitive time lag
ϕ = phase

Subscripts
drop = related to the droplet
inj = at injection
no oscil = under nonoscillatory conditions
oscil = under oscillatory conditions
p = related to pressure
peak = corresponding to the highest value of the response factor
surf = at the droplet surface
u = related to velocity
unif = under spatially uniform conditions (see text)
∞ = at infinity for the droplet

Diacritics
$'$ = fluctuation
$\bar{}$ = mean value

Introduction

THE response of cryogenic rocket engines to combustion instability is known to differ significantly from that of storable propellant engines[1]; cryogenic rocket engines are reputedly more stable than storable propellant engines. The fact that no convincing explanation for this difference has been proposed so far indicates the deficiency of our understanding of liquid rocket combustion instability. The objective in this work is to investigate some of the features that are specific to most cryogenic rocket engines, namely, near-critical ambient conditions and the resulting droplet secondary atomization, and how they affect the response to oscillatory (pressure and velocity) conditions.

To place the present contribution in perspective, a summary of relevant previous works is proposed. However, comprehensive reviews of this topic exist[1,2] and should be consulted for complete information. The first models of liquid rocket combustion instability based on the actual physicochemical droplet processes are due to Strahle,[3–7] Priem and Heidmann,[8] Priem and Guentert,[9] Priem,[10] and Heidmann and Wieber.[11] Priem[9,10] first showed that the stability was affected by vaporization and could be controlled by varying the characteristics of the vaporization process. However, the complexity and validity of these models were restricted by the limitations of the computers available at that time. Recently, Nguyen and Muss[12] proposed an extension of the Agosta–Hammer vaporization response model that is an evolution of the model used by Priem. They tested the influence of various droplet heat transfer modeling options on the predicted vaporization response to mixed radial and tangential modes. The infinite conductivity model (uniform temperature) yielded the best fit with their experimental data. Tong and Sirignano[13] were the first to consider fully the droplet thermal inertia. Their model showed that if

Presented as Paper 93-0231 at the AIAA 31st Aerospace Sciences Meeting and Exhibit, Reno, NV, Jan. 11–14, 1993; received March 10, 1994; revision received May 23, 1995; accepted for publication Aug. 14, 1995.

*Research Associate, Department of Mechanical and Aerospace Engineering. Member AIAA.
†Professor of Mechanical and Aerospace Engineering, Department of Mechanical and Aerospace Engineering. Fellow AIAA.

droplet vaporization is the controlling mechanism, self-sustained acoustical oscillation can occur in the combustion chamber.[2] Several other analyses for vaporization response of droplets have been performed. Bhatia and Sirignano,[14] and Duvvur et al.[15] have examined hydrocarbon droplets in an oscillatory domain. Under certain conditions they predicted combustion chamber instability. Also, see the discussion in Sirignano et al.[2]

The early work of Wieber[16] on high-pressure liquid oxygen droplet vaporization emphasized the possible role that a near-critical condition could play in liquid-rocket combustion instability. Various researchers have improved on Wieber's work, most of them in the domain of hydrocarbon fuel.[17-22] Simulations by Yang and co-workers[22] of pressure-coupled vaporization at supercritical conditions for hydrocarbons burning in air show that the vaporization response changes significantly when the critical mixing conditions are reached. However, the approach chosen to compute the mass flux at the critical interface is not described. Furthermore, their model is spherically symmetric (no convection), neglecting relative velocity effects that are believed to be predominant. Only recent contributions[23,24] deal with the case of a liquid oxygen (LOX) droplet vaporizing at high pressure. Litchford and Jeng[23] used the quasisteady film theory developed for subcritical droplet vaporization and the appropriate high-pressure phase equilibrium relations. They found that the droplet surface can reach the critical state for reduced ambient pressure slightly above one. They indicated that secondary atomization, if it occurred, would seriously affect their conclusions, but they did not include this phenomenon in their model.

In the present work, an open-loop system is considered where the oscillatory gaseous flowfield is imposed and the vaporization response of the droplet array is evaluated. To evaluate the combustion chamber instability, we close the loop following the analysis of Crocco and Cheng[25] by assuming concentrated combustion at the injector end, short nozzle, and isentropic flow downstream of the combustion zone. Since it was recently shown that most droplets in cryogenic rocket engines are likely to undergo secondary atomization in the stripping regime,[26] this phenomenon is included in the analysis. Surface tension is the principal force maintaining drop cohesion. This force vanishes as the surface of a liquid drop approaches the critical conditions. Hence, perturbations induced by the gas relative motion at the drop surface are more likely to grow. Consequently, waves form on the drop surface and are eventually stripped off as a mist of droplets. These droplets are one to two orders of magnitude smaller than the parent drop. Most of them are trapped in the wake of the parent drop and, therefore, affect its heat and mass transfer behavior.

First, isolated droplets are considered. The conditions (temperature, pressure, and velocity) experienced by each droplet in the array are unaffected by the other droplets. The response of the equivalent stream is evaluated by proper integration over the behavior of a given number of drops. A wide range of frequencies is covered and the influence of pressure fluctuation relative amplitude and mean pressure value is investigated. The possibility of droplet gasification being a driving mechanism for liquid-rocket combustion instability is discussed.

The effect of the nonuniformities introduced in the ambient gas flow by the surrounding droplets on the conclusions previously drawn is evaluated. To this end, the idealized droplet array configuration developed previously[27,28] is utilized. Droplets are successively injected in the chamber where they vaporize and burn, modifying the environment of the other droplets. It is emphasized that the simplified droplet array configuration is not meant to simulate an actual combustion chamber. Performing actual combustion instability computations requires an advanced computational fluid dynamics solver to simulate appropriately the behavior of the continuous phase (possibly including turbulent mixing and detailed chemical kinetics). This is not within the scope of this work. It is intended, however, to further the current comprehension of combustion instability mechanisms in liquid rockets by evaluating, in a few idealized cases, how the response of a droplet in the array is affected by indirect interactions between drops and by supercritical conditions.

Model

A standard pressure standing wave is considered. The speed of sound is evaluated at a reference temperature equal to the average temperature in the combustor under nonoscillatory conditions (2000 K in the base case). The velocity fluctuations are easily deduced from the pressure expression if both viscous and inertia terms are neglected in the momentum equation.[29] The temperature fluctuation is related to the pressure fluctuation through an isentropic flow assumption. A few calculations are performed where x is frozen. Then a sinusoidal variation in the ambient conditions of the droplet occurs.

Droplet Transcritical Gasification Model

Similarly, reference is made to Refs. 27 and 30 concerning the details of the model used to compute phase-equilibria at high pressures. Droplet behavior is predicted by numerical solution of the adequately simplified transport equations. The models used have been extensively described elsewhere[26-28,30] and will only be outlined here.

Phase-equilibria are evaluated by solution of the equation system expressing the continuity of temperature, pressure, and fugacity for each component in each phase at the interface. Fugacities are derived from the Redlich–Kwong equation of state with quantum gas mixture rules.[30] The droplet vaporization model is based on the extended film model of Abramzon and Sirignano.[31] A spherically symmetric energy equation is solved to determine the temperature inside the droplet. Possible effects of internal circulation are included through the effective diffusivity model.[31] Because of the reduced surface tension resulting from the vicinity of critical conditions, most droplets in a cryogenic rocket engine undergo secondary atomization in the stripping regime.[26] An expression for the rate of atomization is obtained assuming that it equals the mass flow rate in the liquid boundary layer at the droplet surface. An integral analysis[32,33] of the coupled gas–liquid boundary layers at the droplet surface including blowing effects yields

$$\dot{m}_{\mathrm{BLS}} = \pi D \left(\int_0^{\infty} \rho_l u_l \, \mathrm{d}y \right) = 3\pi R \hat{\rho}_l \Delta U_{\infty} A \alpha_l \sqrt{\frac{\pi R}{2}} \qquad (1)$$

where A (the nondimensional interfacial velocity) and α_l (a liquid boundary-layer velocity profile parameter) are functions of the droplet size, its velocity relative to the gas, and gas and liquid properties.[26] Stripping has been shown[26] to preclude the surface of a vaporizing droplet from reaching the critical mixing conditions in a supercritical environment. In a combustion situation, the surrounding temperature can be high enough for the droplet surface to reach the critical mixing conditions despite the occurrence of stripping. In both cases, secondary atomization in the stripping regime was shown to control the droplet lifetime and to reduce it by one order of magnitude.[26] The stripped liquid is also vaporizing and affects the heat and mass transfer to the parent droplet. A corrected heat transfer number was defined[26] to incorporate this effect,

$$\tilde{B}_T \equiv \frac{\hat{C}_{p_{g,O_2}}(T_{\infty} - T_S) + E_{\mathrm{mist}}/\dot{m}}{\overline{\Delta H}_v(T_S) + Q_l/\dot{m}} \qquad (2)$$

where E_{mist} is a correction to the driving potential due to the presence of the mist.[26] However, most of the stripped liquid vaporizes outside the film due to advection. The source and sink terms in the gas-phase energy and species equations were corrected to include the effect of stripped liquid vaporization.[28]

Response Factor

Simply stated, for a given mechanism to be driving combustion instabilities, it must 1) contribute to the instability and 2) do so in a way sufficient to overcome the losses of the damping processes in the chamber. Evaluating the latter could involve a comprehensive simulation of a liquid-rocket combustion chamber (supercritical, viscous, compressible, unsteady, turbulent, reactive, and three-dimensional flow). The present work focuses on the response of a droplet gasifying in the transcritical mode in an open-loop system; previous theoretical works[1,25] provide an order of magnitude of the response factor values at the stability limits.

The first issue, determining if the mechanism amplifies or damps the instabilities, is classically assessed using the Rayleigh criterion, which states that an initially small pressure perturbation will grow if the considered process adds energy in phase (or with a small enough phase lag) with pressure. To quantify this criterion in the case of droplet vaporization studies, a response factor G was defined,[1,11,13,34]

$$G = \frac{\iint \dot{W}' p' \, dt \, dz}{\iint p'^2 \, dt \, dz} \tag{3}$$

where the primes denote fluctuations with respect to the mean, or nonoscillatory, values. Embedded in this definition is the assumption that the characteristic times for mixing and chemical reaction are significantly smaller than those for gasification, so that the gasification process is rate controlling.[13] That is, the energy release rate is well approximated by the gasification rate.

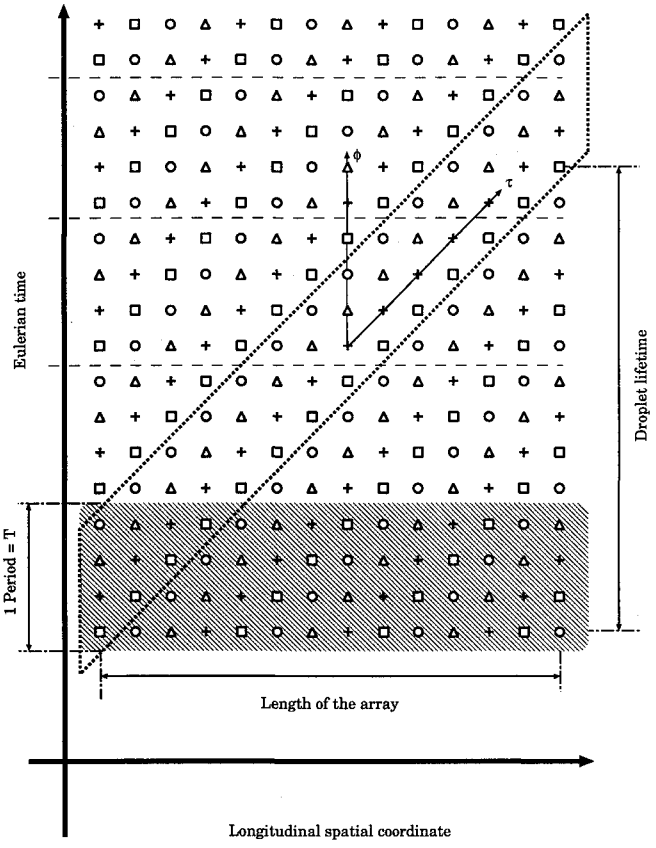

Fig. 1 Response factor integration. □: droplet injected at $t = 0$, $\phi = 0$; +: droplet injected at $t = T/4$, $\phi = \pi/2$; △: droplet injected at $t = T/2$, $\phi = \pi$; ○: droplet injected at $t = 3T/4$, $\phi = 3\pi/2$.

In a normalized fashion, G is the magnitude of the Fourier component of vaporization rate (burning rate) that is in phase with the sinusoidal pressure oscillation. This interpretation applies even when the nonlinearities in the droplet vaporization model are considered. The use of G later in this analysis, together with the linearized representation of the chamber effects, is tantamount to a process of equivalent linearization whereby the relevant aspects of the nonlinear behavior are represented by means of the primary Fourier component.[35]

If $G > 0$ ($G < 0$), the gasification process has a destabilizing (stabilizing) tendency. However, G must exceed a threshold value for instability to result. If concentrated combustion is assumed at the injector end, it can be shown that $G(f)$ must be larger than $(\gamma + 1)/2\gamma$. This value may be obtained from a simple analysis estimating the potential acoustic losses from the exhaust nozzle,[34] or using the more detailed sensitive time-lag theory.[1,25] An appropriate average value of γ was selected. For a mixture of oxygen, hydrogen, and water at 100 atm and 1500 K ($C_{p_{O_2}} = 1.1$ kJ/kg K, $C_{p_{H_2}} = 15.5$ kJ/kg K, and $C_{p_{H_2O}} = 2.44$ kJ/kg K), γ ranges from 1.23 (pure H_2O) to 1.37 (pure H_2). For a typical composition ($Y_{O_2} = 0.2$, $Y_{H_2} = 0.2$, and $Y_{H_2O} = 0.6$), $\gamma = 1.32$. Therefore $(\gamma + 1)/2\gamma = 0.88$.

In the configuration considered here, the level of idealization is such that this definition [Eq. (3)] cannot be used directly. It should be noted that, in a real combustion chamber, the injection process is continuous. Hence, for any value of the phase angle ϕ and at any given instant, there exists in the combustion chamber a droplet that was injected at a time corresponding to ϕ. Consequently, the integrals over Eulerian space and time in Eq. (3) may be replaced by integrals over Lagrangian time τ and the phase at injection ϕ (cf. Fig. 1). Therefore,

$$G = \frac{\oint\!\!\int \dot{W}' p' \, d\tau \, d\phi}{\oint\!\!\int p'^2 \, d\tau \, d\phi} \tag{4}$$

Note that a similar summation process to evaluate the response factor was used by Heidmann and Wieber.[34]

Validity of the Concentrated Combustion Assumption

The combustion chamber stability is evaluated using a concentrated combustion assumption, whereby all of the elements of propellant are being consumed at the injector face. Crocco and Cheng[1,25] showed that the stability behavior could be extremely sensitive to the position of the combustion front and that combustion distribution might significantly affect the stability characteristics. However, this approximation seems reasonable here given the short droplet lifetime (single combustion front at $z = 0$). A simplified analysis[36] shows that a correction for the distribution of the combustion process will not change the conclusion about the instability for the current propellant configuration under study.

If distributed combustion is considered, the flowfield is no longer uniform, and mass, momentum, and energy sources are distributed in the chamber. Crocco and Cheng[36] computed the threshold response factor for instability in the particular case of a linear mean velocity profile from injection to ξ_c and uniform thereafter. In these computations, they neglected the damping effects of the droplets (drag) and assumed a Mach number of 0.213 for the flow entering the nozzle. They found that reaction zone spreading is stabilizing. The maximum threshold value of the interaction index for unstable operations with uniformly distributed combustion is about three times larger than the corresponding value for combustion concentrated near the injection point. However, for ξ_c under 0.2 (10 cm for a 0.5-m-long chamber) the threshold response factor for instability is barely affected by combustion distribution, so that the value for combustion concentrated at the injector face

could be used in this case. Previous evaluations[27,28] of the reaction zone spreading in the configuration considered here showed that it is well below 10 cm, validating the concentrated combustion assumption. In this configuration $M \simeq 0.08$. However, at low Mach number the threshold response factor for instability is not significantly affected by the actual value of M. It is therefore legitimate to use the results of Crocco and Cheng to obtain a qualitative evaluation of the concentrated combustion assumption.

Results and Discussion

Reference Case

The gasification response of an LOX droplet in an oscillatory environment is evaluated. In the reference case, $\bar{T}_\infty = 1000$ K, $\bar{P}_\infty = 100$ atm, $\bar{U}_\infty = 120$ m/s, and the LOX droplet is injected at 100 K with a relative velocity of 20 m/s. $\varepsilon_P = 0.02$, yielding $\varepsilon_U = a\varepsilon_P/(\gamma\bar{U}_\infty) \simeq 0.1$ and $\varepsilon_{\Delta U} = a\varepsilon_P/(\gamma\overline{\Delta U}) \simeq 0.6$, if the inertial terms are neglected in the momentum equation. A wide frequency spectrum is covered (250 Hz to 50 Hz). For each case considered the corresponding nonoscillatory case is also evaluated.

In Fig. 2, the conditions in the gas (at infinity for the drop), droplet radius, surface temperature, and gasification rate histories are plotted. All fluctuations are evaluated with respect to the value of the corresponding quantity at the same time in nonoscillatory conditions. These normalized fluctuations are not those used in the response factor computations. This type of normalization is used for all plots of fluctuations in this article. Note the top graph in Fig. 2 shows the conditions seen by the droplet as it moves through the standing wave. The gasification rate is primarily affected by the fluctuations of the gas velocity (10% mean to peak), which causes relative velocity oscillations with a relative amplitude ($\varepsilon_{\Delta U} = \varepsilon_U\bar{U}_\infty/\overline{\Delta U}$) of 0.6 and gasification rate fluctuation with a relative amplitude up to 0.3. The surface temperature does not reach the critical mixing value and, as the ambient pressure oscillates, the corresponding equilibrium conditions change at the droplet surface; thus the surface temperature oscillates. For the cases investigated here, the fluctuations in critical mixing temperature were below 1% (mean to peak). Therefore, these fluctuations had a negligible effect on the gasification rate response. Relative velocity effects are usually dominant. To obtain a good phase resolution the gasification response of 16 droplets (injected every $\pi/8$) is computed for each frequency considered.

Figure 3 shows the computed response factor G vs frequency f. At 11 kHz G peaks with a value of 1.67. This frequency corresponds to a time period of 90.91 μs, i.e., a ratio to the average droplet lifetime (τ_p/t_{life}) of 0.4. On average (over the spectrum), the gasification process is contributing to the instabilities; G is positive over a fairly wide range of frequencies. Furthermore, the response factor is above $(\gamma + 1)/2\gamma = 0.88$ (horizontal dash–line in Fig. 3) for frequencies between 7–14 kHz. It is therefore concluded that, under the conditions considered here, the gasification process has a response factor large enough to drive the instability in this range.

Response Spectrum Analysis

To understand which factors determine the peak frequency and what causes the secondary peak, the velocity, pressure, and gasification rate fluctuation histories for the base case at 2, 11, and 30 kHz are plotted in Fig. 4. Two particular droplets are shown with phase angles at injections of $5\pi/8$ and $3\pi/2$. It is not possible to extrapolate the behavior of the elementary response factor from such plots; however, these are helpful to understand the basic phenomena. Figure 4 shows that the important parameter is the ratio of the droplet lifetime to the largest time period T^* of the wave pattern displayed. The observed wave pattern results from the composition of the droplet motion and the imposed

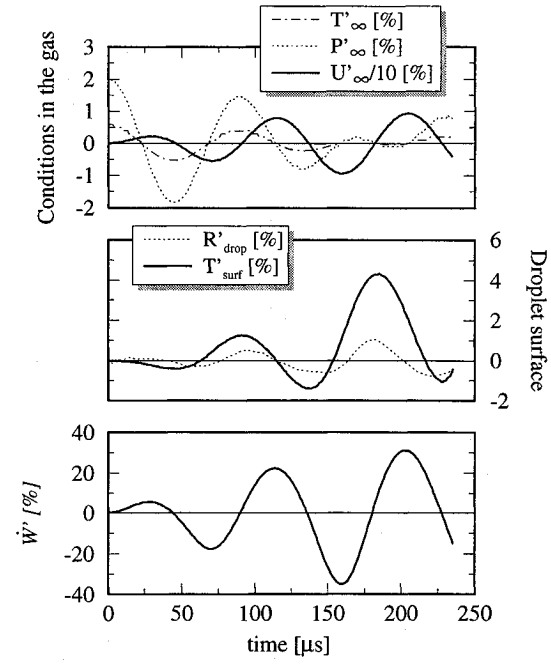

Fig. 2 Isolated LOX droplet vaporizing in an oscillatory field. Base case with f = 11 kHz, ε_P = 0.02, phase at injection: 0.

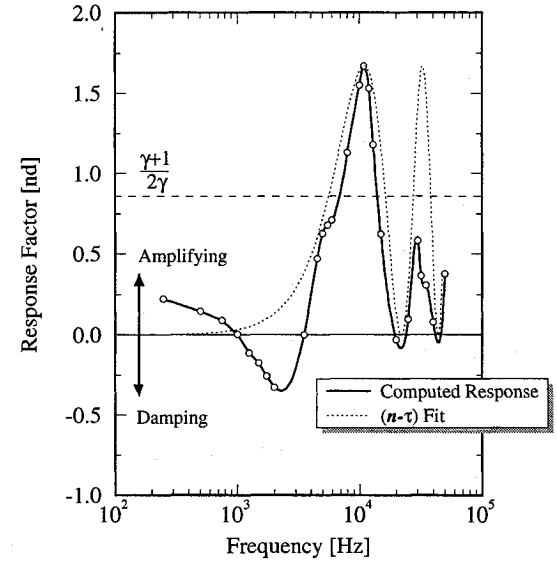

Fig. 3 Response factor for an isolated LOX droplet with stripping. $\bar{T}_\infty$ = 1000 K, $\bar{P}_\infty$ = 100 atm, $\bar{U}_\infty$ = 120 m/s, $\bar{V}_{drop}|_{t=0}$ = 100 m/s, and ε_P = 0.02.

standing wave. This is clearer if the droplet position is approximated by $\bar{U}_{drop}(t - t_{inj})$, where $\bar{U}_{drop}$ is an average droplet velocity. The fluctuations are then proportional to

$$\cos[2\pi(\bar{U}_{drop}/a)f(t - t_{inj})] \times \cos(2\pi ft) \quad (5)$$

with a beating period of $T^* \simeq aT_p/\bar{U}_{drop}$. In the base case reported here, $\bar{U}_{drop}/a \simeq 0.1$. It was observed that the ratio of the forcing oscillation time period to the droplet lifetime was about 0.4, this corresponds to $t_{life}/T^* \simeq 1/4$, as can be verified in Fig. 4. For smaller forcing frequencies (larger T^*), the droplet experiences only a fraction of the potential velocity fluctuation. $t_{life}/T^* \simeq \frac{3}{4}$ logically corresponds to a local maximum for the response; thus, the secondary peak occurs at about three times the peak frequency.

The interaction index n and the time lag τ corresponding to this response can be evaluated.[11] Figure 3 shows the resulting

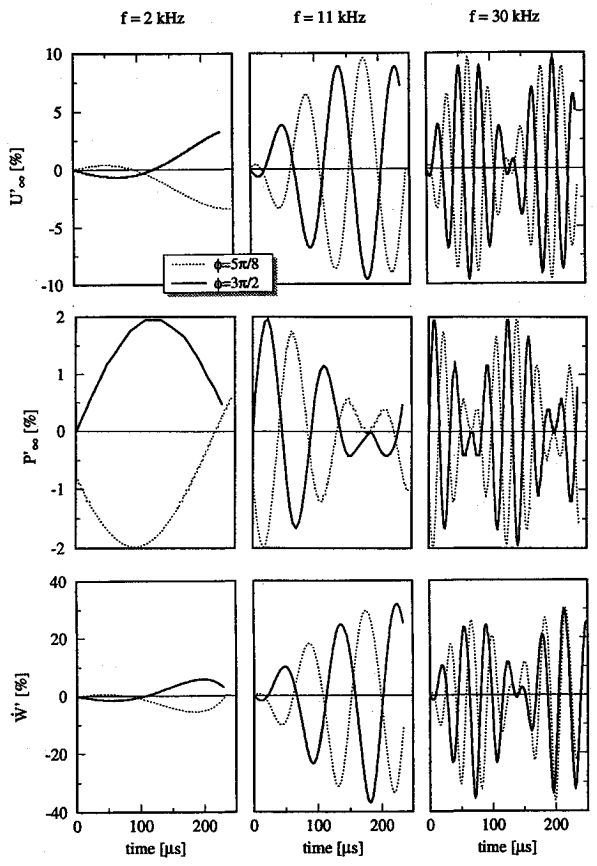

Fig. 4 Velocity, pressure, and gasification rate fluctuation histories for the base case.

plot for $n = 0.835$ and $\tau = 45.5$ μs. Note that the $(n - \tau)$ response also exhibiting a secondary peak at about 25 kHz is a coincidence. Indeed, a more elaborate development of the sensitive time-lag theory shows only the first peak.[1] It is also emphasized in this analysis that the full nonlinear droplet heating, gasification, and drag mechanisms are considered. When linearization is used, it leads to neglecting these terms that were shown to be extremely important here. This indicates the limitations of a perturbation analysis.

Influence of Pressure Fluctuation Relative Amplitude

To investigate the effect of flow reversal on the response factor spectrum, a case with a pressure fluctuation relative amplitude of 0.1 is considered. The corresponding ε_u is about 0.5, which is sufficient for flow reversal to occur since in this case the mean relative velocity is 20% of the mean gas velocity. The computed response factor spectrum is plotted in Fig. 5. The base case response factor spectrum is shown for comparison.

It is noted first that the overall effect of a higher ε_P is a shift in the peak frequency from 11 to 5.5 kHz. Furthermore, the secondary peak is relatively higher (the secondary peak height is 63% of the main peak's height, whereas it is only 36% for $\varepsilon_P = 0.02$). Moreover, the secondary peak occurs at about twice the peak frequency (and not three times as in the base case). This frequency shift is due to the change in wave pattern that the droplet experiences due to flow reversal and the resulting change in the instantaneous gasification rate fluctuation history (see Fig. 6). The changes in the response factor spectrum induced by variations of the pressure fluctuation relative amplitude are clearly nonlinear. Therefore, a perturbation analysis (linearized) would not predict them correctly.

Response of Droplets Not Undergoing Secondary Atomization

In this section, the effects of stripping on the previously drawn conclusions are evaluated by comparison with cases

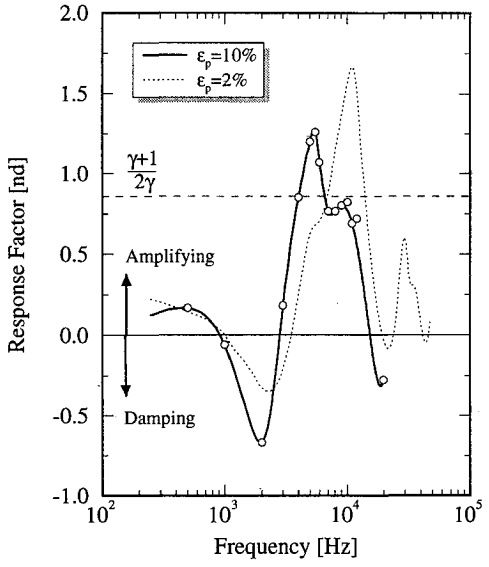

Fig. 5 Influence of the pressure fluctuation relative amplitude on the response factor.

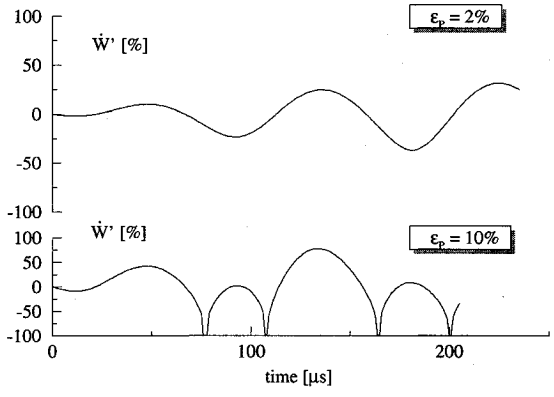

Fig. 6 Effect of flow reversal on the instantaneous gasification rate fluctuation history.

where stripping is not included, all other parameters being unchanged. The major differences in terms of the response of one droplet are dictated by the characteristics already observed under nonoscillatory conditions.[26,27] The droplet lifetime is much larger here (about 4.6 ms) due to the gasification rate being more than one order of magnitude smaller than when stripping is included. The droplet surface temperature reached the critical mixing conditions in all of the cases without stripping covered. The pressure oscillations have a secondary effect here in their influence on the critical mixing conditions and thereby on the droplet surface temperature. However, this is completely overshadowed by the velocity fluctuations and their convective effects.

The resulting response factor is plotted vs f in Fig. 7, together with the response spectrum obtained with stripping (mixed line). The most important feature is the frequency shift of the peak that is now located at 500 Hz, with a maximum value of 2.3. Nevertheless, this peak frequency still corresponds to a time period to droplet lifetime ratio of about 0.4, as in the stripping case. The secondary peak is found at 1500 Hz, three times the peak frequency as in the case with stripping; this is also attributed to the smaller characteristic times introduced by the flow reversal towards the end of the droplet lifetime. In this case, the peak is narrower, but the maximum reached is higher (38%). The computed response factor value is above the concentrated combustion threshold limit $(\gamma + 1)/2\gamma$ for frequencies between 250–700 Hz. Therefore, it is in-

ferred in this case too that the gasification process has a response factor sufficiently large to drive the instability in the limited range reported.

In this case, the droplet lifetime (and therefore the peak frequency) is controlled by the regression of the critical interface (cf. Refs. 26 and 30). The value of the mean pressure should consequently be an important factor. The most dramatic effects are expected when the mean pressure is so low that the droplet surface temperature does not reach the critical conditions and undergoes usual (albeit high pressure) convective vaporization. In Fig. 8, the base case without stripping is compared to a case where $\bar{P} = 43$ atm, everything else being unchanged. Under these conditions, the droplet surface does not reach the critical mixing conditions. Its lifetime is influenced more by the relative velocity than in the transcritical cases and is about 50% shorter (from 4.5 to 2.4 ms). Accordingly, the peak frequency is shifted from 500 to 800 Hz, and the peak value (at 2.73) is more than 50% higher than the peak value for transcritical conditions (1.75). This suggests that the transcritical regime (without stripping) is more stable. Note, however, that the effect of the mean pressure value is a lot less significant when stripping is included (a partial plot is provided in Fig. 8 for comparison) and that, in this case, higher-pressure yields larger response factors, indicating a destabilizing effect.

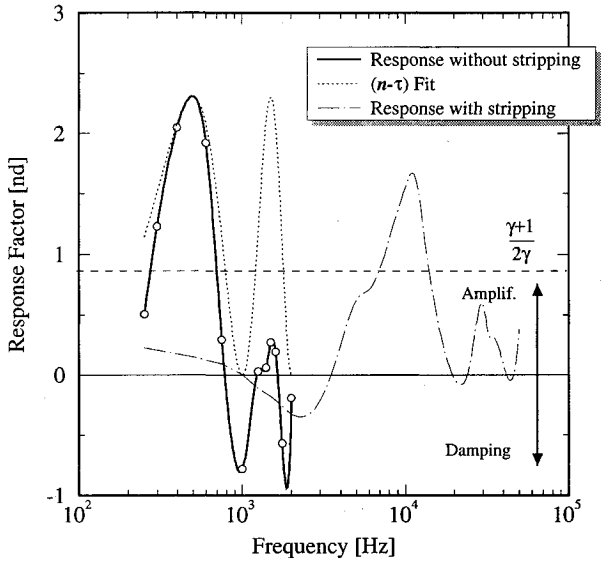

Fig. 7 Response factor for an isolated LOX droplet without stripping. $\bar{T}_\infty$ = 1000 K, $\bar{P}_\infty$ = 100 atm, $\bar{U}_\infty$ = 120 m/s, $\bar{V}_{drop}|_{t=0}$ = 100 m/s, and ε_P = 0.02.

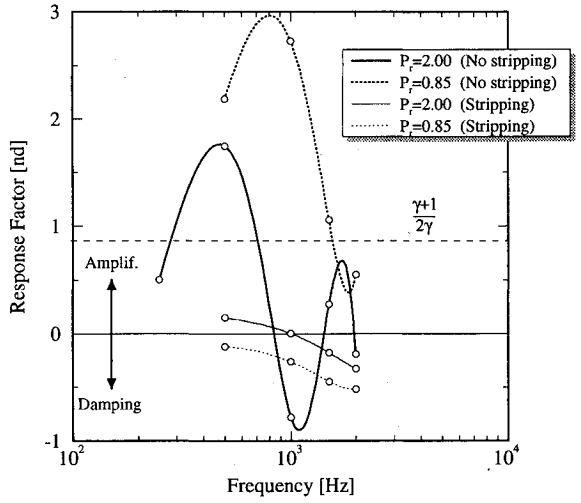

Fig. 8 Influence of the mean pressure on the response factor.

Influence of Neighbor-Induced Gas Field Nonuniformities

As mentioned previously, the parallel-stream configuration is not meant to simulate instabilities in a real combustion chamber; it is rather an extension of the isolated droplet model used in the previous section that allows the inclusion of indirect droplet interaction effects on the response of a droplet in an array to a prescribed oscillatory gaseous flow.

In the base case considered, LOX droplets with an initial diameter of 100 μm and an initial temperature of 100 K are injected in a mixture of hydrogen (Y_{H_2} = 0.2) and water vapor (Y_{H_2O} = 0.8), initially at 1000 K. The chamber pressure is uniform at 100 atm, the gas injection velocity is 1 m/s, and the droplets are injected at 21 m/s; stripping is included. The computational domain is 1.5 cm long by 0.125 cm wide. Using higher gas velocity, such as that considered in the cases reported earlier, would require a much larger domain and significantly more droplets, and therefore, unrealistically increasing the computational load. The main purpose here is to establish a comparison with the isolated droplet computations. Therefore, it is necessary to approach continuous injection. In the case considered, the isolated droplet cases suggest that interesting frequencies should be around 10 kHz. At least five droplets per cycle are needed to obtain a not-too-coarse discretization of the phase interval. Hence, the injection frequency must be at least 50 kHz; then the droplet spacing is roughly four droplet diameters and the equivalence ratio is 5.14. At t = 1.4 ms, after the initial transient, the chamber pressure is perturbed following a standing wave pattern with a frequency of 10 kHz. The pressure fluctuation relative amplitude is ε_P = 0.02. The gas-phase velocity perturbation is obtained as in the isolated droplet case; but, because ε_U is proportional to $1/\bar{U}_\infty$, the gas velocity fluctuation relative amplitude can be as high as 12. However, the relative velocity fluctuation relative amplitude $\varepsilon_{\Delta U}$ remains of the same order as in the cases reported earlier ($\simeq$0.6), since $\overline{\Delta U}$ is unchanged at 20 m/s. Note that neglecting the inertial terms (which leads to an error of order M in the perturbation equations) might be questionable in real rocket engines. However, here, the Mach numbers considered are all less than 0.1. Furthermore, if the inertial terms were to be included, an ordinary differential equation with complex variable coefficients would have to be solved at each time step and each longitudinal location to evaluate the velocity fluctuation, which would increase the computational load even further. The mean value of the gas velocity is evaluated through a mass balance as described in Refs. 27 and 28, so that $\bar{U}$ is a function of the longitudinal location z.

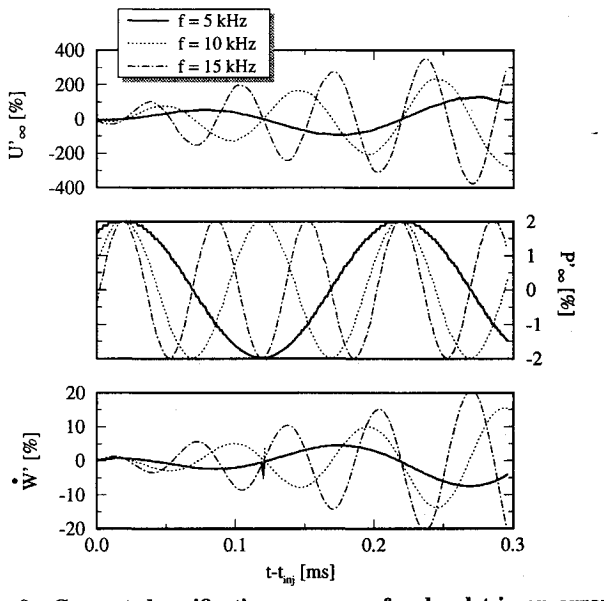

Fig. 9 Computed gasification response of a droplet in an array at 5, 10, and 15 kHz.

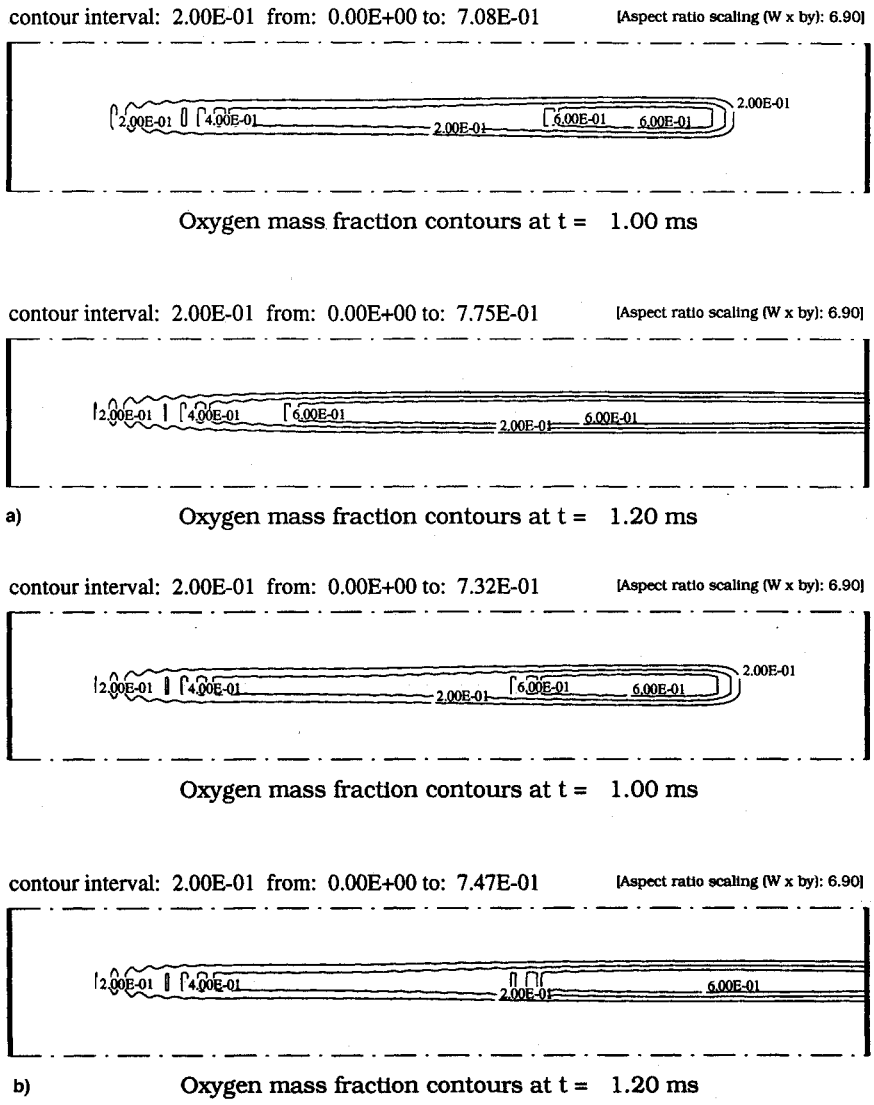

Fig. 10 Array of LOX droplets with an initial diameter of 150 μm injected at 60 m/s. Gas injection velocity: 40 m/s. Computational domain: 7.4 × 0.185 cm. The equivalence ratio is 5.14: a) oxygen mass fraction contours, at and after the onset (t = 1 ms) of the pressure perturbation and b) in the nonoscillatory case at 1 and 1.2 ms.

Figure 9 shows the gasification rate fluctuation history as well as the gas velocity and pressure fluctuations experienced by a droplet in the base case at 5, 10, and 15 kHz. Here again, it is clear that the velocity fluctuations are predominant in the determination of the gasification response. The pressure experienced by the droplet is almost sinusoidal because the ratio of the droplet velocity to the sound velocity is small ($T^* << T$). For larger frequencies (smaller T), the standing wave pattern is more discernible. The small inaccuracies that can be observed on the computed gasification rate fluctuations are caused by small instantaneous relative velocities where the breakup criterion is marginally satisfied.

At the onset of the oscillations (1 ms), the mean longitudinal velocity experiences a transient increase. Eventually, the exit velocity is about 30% higher than the corresponding nonoscillatory value. The mean longitudinal velocity profiles (not shown) indicate that this increase occurs in a region between 2–5 cm from the inlet. Comparison of the oxygen mass fraction contour plots at 1 and 1.2 ms, in both this oscillatory case (Fig. 10a) and the corresponding nonoscillatory case (Fig. 10b), shows that gasification is enhanced in that region (from 2 to 4 cm). Indeed, z = 28 mm corresponds roughly to a velocity antinode under the conditions considered here. Since velocity effects are predominant in the oscillatory vaporization results, this effect of oscillatory ambient conditions on the mean longitudinal velocity is extremely significant in terms of gasification rate response.

Isolated Droplet vs Droplet in an Array Response Comparison

The predicted response of a droplet in an array (base case) is compared to that of an isolated droplet vaporizing at the same conditions in Fig. 11. Note that the fluctuations plotted in these figures are normalized by the instantaneous value of the considered quantity, computed for the same droplet in nonoscillatory conditions, so that what is compared here is the difference between the departures from the nonoscillatory behavior only. Furthermore, even though the gas velocity fluctuation U'_∞ can be as high as 2.0 (cf. Fig. 11), the relative velocity fluctuation relative amplitude is still of the order of 0.6, which explains that the gasification rate fluctuation relative amplitude is of the same order as that shown in Fig. 2.

The array configuration and the isolated droplet configuration are significantly different. In the array configuration, the droplets go through a reaction zone and the local species concentration and the relative velocity experienced by the droplets are influenced by the neighboring droplets. The difference in mean relative velocity results in a slight reduction of the stripping rate and a longer lifetime predicted for droplets in the array configuration. However, the effect on the relative velocity fluctuation is relatively minor and the computed responses

Table 1 Comparison of the response factors obtained by the isolated droplet method and the droplet in an array method[a]

f, kHz	Isolated drop[b]	Drop array[b]	Uniform response factor
5	0.217 (16)	0.425 (12)	0.1075
10	0.221 (16)	0.411 (6)	0.1077
15	0.273 (16) 0.739 (4)	0.726 (4)	0.1082

[a]The uniform response factor values are shown for reference.
[b]The numbers in parentheses indicate the number of droplets per cycle.

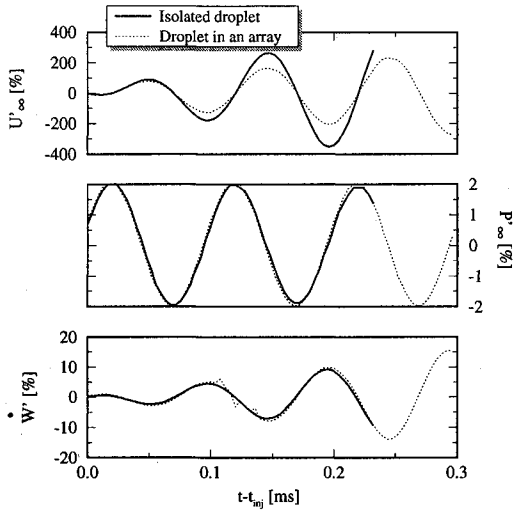

Fig. 11 Comparison of the predicted isolated droplet response to an oscillatory field (10 kHz) with the predicted response of the same droplet in an array ($\phi = 8\pi/5$).

almost coincide (they differ only by a few percents and a small phase lag). This is consistent with the observation made previously concerning the importance of relative velocity fluctuations. Note that the effect of the reaction zone in the array configuration, resulting in higher droplet temperature, is insignificant since the stripping rate is mechanically, rather than thermally, controlled.[26,27]

The computed response factors in both configurations are compared in Table 1. In the array configuration, the Eulerian expression of the response factor may be used. The chemical conversion rate is available in this configuration. However, the limitations imposed on the mesh size by the point-source approximation yield a poor resolution of the reaction zone. The droplet response is mechanically controlled (stripping) rather than thermally, and therefore is not significantly affected by these inaccuracies. Hence, the gasification rate is still assumed to be controlling and is used to compute the response factor. The computed thickness of the reaction zone, even though it is overestimated, indicates a very fast chemical reaction, therefore validating this assumption. For the three frequencies considered, the response factor in the array configuration was always larger than that obtained with the isolated droplet configuration. However, because of computational limitations, continuous injection cannot be approached in the array configuration as well as with the isolated droplet model. For instance, at 15 kHz, only four droplets per cycle could be used. If only four droplets per cycle are used with the isolated droplet model, the computed response factor becomes 0.74, which compares well with the value obtained in the array configuration at 15 kHz. At lower frequencies, the numbers of droplets used become comparable and the higher response factor observed in the array configuration is attributed to the longer droplet lifetime.

The response factor resulting from a perturbation analysis (as defined by Crocco[1]) was also computed for comparison purposes. Note that in the derivation of this quantity the complex combustion response factor is assumed to be uniform. In the present study, however, the response factor is not uniform. Using this expression therefore amounts to using an average value for the complex combustion response factor in its derivation. In these computations, the damping effects of the droplets (drag) and the nozzle were not included for consistency with the other response factors computed here, the expression is therefore,[1]

$$G_{\text{unif}} = \frac{-(2-\gamma)\pi/L \int_0^L \bar{U}_g(x)\sin(2\pi x/L)\,dx}{\gamma\left[\bar{U}_g(L) + \pi/L \int_0^L \bar{U}_g(x)\sin(2\pi x/L)\,dx\right]}$$

The values obtained for G_{unif} are much lower than those obtained by the two other methods (cf. Table 1). These discrepancies are attributed to the previously mentioned differences in the assumptions of the models resulting from their different goals. In this study a better understanding of the factors controlling the droplet gasification response is sought, so that the domain investigated is fairly small. Models such as the $(n-\tau)$ model aim at providing a prediction of the response of the whole combustion chamber. The use of linearization and perturbation methods results in an oversimplification of the actual vaporization process.

Conclusions

It was shown that the gasification process has enough potential to drive longitudinal mode combustion instabilities, under the simplifying assumptions used in this work. Furthermore, the peak frequency for the computed response factor is correlated to the droplet lifetime. Therefore, secondary atomization, which causes a substantial reduction of the droplet lifetime (one order of magnitude), results in a significant shift of the peak frequency, away from the common modes for standard rocket engines. This phenomenon could explain the observed better stability of cryogenic rocket engines relative to storable propellant rocket engines, since, for cryogenic propellants, most droplets are likely to undergo secondary atomization in the stripping regime.

A secondary peak in the response function was identified and linked to both the magnitude of the droplet velocity to sound velocity ratio and the possible occurrence of flow reversal. The effects of relative velocity fluctuations are predominant and cannot be overlooked in combustion instability studies. Effects of pressure fluctuations on the critical interface location appear to be minor in the cases investigated. Supercritical mean pressures have mixed effects: destabilizing for droplets undergoing secondary atomization, but stabilizing for the others.

The comparison of the values computed in both configurations indicates that the response spectra obtained with the vaporizing isolated droplet configuration underestimate the driving potential of the gasification process. It is emphasized, however, that the array configuration presented here is extremely idealized so that only trends could be obtained.

Acknowledgments

This work was sponsored by Société Européenne de Propulsion (SEP–Vernon, France). The computations were performed on the Convex C-240 (Office of Academic Computing at the University of California, Irvine) and the Cray Y-MP (San Diego Supercomputer Center) through a UCI block-grant. J.-P. Delplanque acknowledges fellowship support from SEP. C. L. Merkle and one of the reviewers provided detailed insightful comments and constructive criticism toward the improvement of this article.

References

[1]Harrje, D. T., and Reardon, F. H. (eds.), "Liquid Propellant Rocket Combustion Instability," NASA SP-194, 1972.

[2]Sirignano, W. A., Delplanque, J.-P., Chiang, C. H., and Bhatia, R., "Liquid-Propellant Droplet Vaporization: A Rate Controlling Process for Rocket Combustion Instability," *Liquid-Rocket Engine Combustion Instability*, edited by V. Yang and W. E. Anderson, Progress in Astronautics and Aeronautics, AIAA, Washington, DC, 1995, Vol. 169, pp. 307–343.

[3]Strahle, W. C., "A Theoretical Study of Unsteady Droplet Burning: Transients and Periodic Solutions," Ph.D. Dissertation, Princeton Univ., Princeton, NJ, 1960.

[4]Strahle, W. C., "Periodic Solutions to a Convective Droplet Burning Problem: The Stagnation Point," *Proceedings of the 10th Symposium (International) on Combustion*, The Combustion Inst., Pittsburgh, PA, 1964, pp. 1315–1325.

[5]Strahle, W. C., "High-Frequency Behavior of the Laminar Jet Flame Subjected to Transverse Sound Waves," *Proceedings of the 11th Symposium (International) on Combustion*, The Combustion Inst., Pittsburgh, PA, 1966, p. 747.

[6]Strahle, W. C., "Unsteady Laminar Jet Flames at Large Frequencies of Oscillation," *AIAA Journal*, Vol. 3, No. 5, 1965, pp. 957–960.

[7]Strahle, W. C., "Unsteady Reacting Boundary Layer on a Vaporizing Flat Plate," *AIAA Journal*, Vol. 3, No. 6, 1965, pp. 1195–1198.

[8]Priem, R. J., and Heidmann, M. F., "Propellant Vaporization as a Design Criterion for Rocket Engine Combustion Chambers," NASA TR-R67, 1960.

[9]Priem, R. J., and Guentert, D. C., "Combustion Instability Limits Determined by a Nonlinear Theory and a One-Dimensional Model," NASA TN D-1409, Oct. 1962.

[10]Priem, R. J., "Theoretical and Experimental Models of Unstable Rocket Combustors," *Proceedings of the 9th Symposium (International) on Combustion*, The Combustion Inst., Pittsburgh, PA, 1963, pp. 982–992.

[11]Heidmann, M. F., and Wieber, P. R., "Analysis of *n*-Heptane Vaporization in Unstable Combustor with Travelling Transverse Oscillations," NASA Technical Rept. TN D-3424, Nov. 1965.

[12]Nguyen, T. V., and Muss, J. A., "Modification of the Agosta-Hammer Vaporization Response Model for the Prediction of High-Frequency Combustion Instabilities," 24th JANNAF Combustion Subcommittee Meeting, Oct. 1987.

[13]Tong, A. Y., and Sirignano, W. A., "Oscillatory Vaporization of Fuel Droplets in an Unstable Combustor," *Journal of Propulsion and Power*, Vol. 5, No. 3, 1989, pp. 257–261.

[14]Bhatia, R., and Sirignano, W. A., "One-Dimensional Analysis of Liquid-Fueled Combustion Instability," *Journal of Propulsion and Power*, Vol. 7, No. 6, 1991, pp. 953–961.

[15]Duvvur, A., Chiang, C. H., and Sirignano, W. A., "Oscillatory Fuel Droplet Vaporization: Driving Mechanism for Combustion Instability," *Journal of Propulsion and Power*, Vol. 12, No. 2, 1996, pp. 358–365.

[16]Wieber, P. R., "Calculated Temperature Histories of Vaporizing Droplet to the Critical Point," *AIAA Journal*, Vol. 1, No. 12, 1963, pp. 2764–2770.

[17]Lazar, R. S., and Faeth, G. M., "Bipropellant Droplet Combustion in the Vicinity of the Critical Point," *11th Symposium (International) on Combustion*, The Combustion Inst., Pittsburgh, PA, 1967, pp. 801–811.

[18]Manrique, J. A., and Borman, G. L., "Calculation of Steady State Droplet Vaporization at High Ambient Pressures," *International Journal of Heat and Mass Transfer*, Vol. 12, 1969, pp. 1081–1095.

[19]Matlosz, R. L., Leipziger, S., and Torda, T. P., "Investigation of a Liquid Drop Evaporation in a High Temperature and High Pressure Environment," *International Journal of Heat and Mass Transfer*, Vol. 15, 1972, pp. 831–852.

[20]Curtis, E. W., and Farrell, P. V., "Droplet Vaporization in a Supercritical Microgravity Environment," *Astronautica Acta*, Vol. 17, No. 11/12, 1988, pp. 1189–1193.

[21]Hsieh, K. C., Shuen, J. S., and Yang, V., "Droplet Vaporization in High-Pressure Environments. 1. Near Critical Conditions," *Combustion Science and Technology*, Vol. 76, Nos. 1–3, 1991, pp. 111–132.

[22]Yang, V., Hsiao, C. C., and Shuen, J. S., "Pressure-Coupled Vaporization and Combustion Responses of Liquid Fuel Droplets in High-Pressure Environments," AIAA Paper 91-2310, June 1991.

[23]Litchford, R. J., and Jeng, S.-M., "LOX Vaporization in High-Pressure Hydrogen-Rich Gas," AIAA Paper 90-2191, July 1990.

[24]Yang, V., Lin, N. N., and Shuen, J. S., "Vaporization of Liquid Oxygen (LOX) Droplets at Supercritical Conditions," AIAA Paper 91-0078, Jan. 1992.

[25]Crocco, L., and Cheng, S. I., *Theory of Combustion Instability in Liquid Propellant Rocket Motors*, Vol. 8, Butterworths, London, 1956.

[26]Delplanque, J.-P., and Sirignano, W. A., "Boundary Layer Stripping Effects on Droplet Transcritical Convective Vaporization," *Atomization and Sprays*, Vol. 4, 1994, pp. 325–349.

[27]Delplanque, J.-P., "Liquid Oxygen Droplet Vaporization and Combustion: Analysis of Transcritical Behavior and Application to Liquid Rocket Combustion Instability," Ph.D. Dissertation, Dept. of Mechanical and Aerospace Engineering, Univ. of California, Irvine, CA, 1993.

[28]Delplanque, J.-P., and Sirignano, W. A., "Transcritical Vaporization and Combustion of LOX Droplet Arrays in a Convective Environment," *Combustion Science and Technology*, Vol. 105, 1995, pp. 327–344.

[29]Williams, F. A., *Combustion Theory*, Benjamin–Cummings, Menlo Park, CA, 1985.

[30]Delplanque, J.-P., and Sirignano, W. A., "Numerical Study of the Transient Vaporization of an Oxygen Droplet at Sub- and Supercritical Conditions," *International Journal of Heat and Mass Transfer*, Vol. 36, No. 2, 1993, pp. 303–314.

[31]Abramzon, B., and Sirignano, W. A., "Droplet Vaporization Model for Spray Combustion Calculations," *International Journal of Heat and Mass Transfer*, Vol. 32, Nov. 1989, pp. 1605–1618.

[32]Ranger, A. A., and Nicholls, J. A., "Aerodynamic Shattering of Liquid Drops," *AIAA Journal*, Vol. 7, No. 2, 1969, pp. 285–290.

[33]Taylor, G. I., "The Shape and Acceleration of a Drop in a High-Speed Air Stream," *The Scientific Papers of G. I. Taylor*, edited by G. K. Batchelor, Vol. 3, Cambridge Univ. Press, Cambridge, England, UK, 1963.

[34]Heidmann, M. F., and Wieber, P. R., "Analysis of Frequency Response Characteristics of Propellant Vaporization," NASA TM X-52195, June 1966.

[35]Minorsky, N., *Nonlinear Oscillations*, D. van Nostrand Company, Inc., New York, 1962.

[36]Crocco, L., and Cheng, S.-I., "High-Frequency Combustion Instability in Rockets with Distributed Combustion," *Proceedings of the 4th Symposium (International) on Combustion*, Williams and Wilkens, Baltimore, MD, 1952, pp. 865–880.